

CONFERENCES AND SYMPOSIA

PACS numbers: **07.57. – c, 74.45. + c,** 85.25.Pb

90th ANNIVERSARY OF THE P.L. KAPITZA INSTITUTE FOR PHYSICAL PROBLEMS
RUSSIAN ACADEMY OF SCIENCES

External factors acting on low-temperature conductivity of superconductor–insulator–normal metal–insulator–superconductor tunnel structures *

S.A. Lemzyakov, M.A. Tarasov, V.S. Edelman

DOI: https://doi.org/10.3367/UFNe.2024.12.039844

Contents

Abstract. **We review the most notable experiments conducted at the Institute for Physical Problems, Russian Academy of Sciences, in cooperation with the Kotelnikov Institute of Radioengineering and Electronics, Russian Academy of Sciences, on the effect that millimeter-wave irradiation, temperature T, and magnetic field B have on the conductivity of superconductor–insulator–normal metal–insulator–superconductor (SINIS) tunnel structures at temperatures $T \ll T_c$ and at low voltages, such that the single-electron current is comparable to or smaller than the subgap two-electron Andreev current. We find that, under irradiation with energy of quanta $\hbar\omega \gg kT$, the normal-metal electron subsystem does not reach equilibrium. Under pulsed irradiation, the time constant of SINIS structures regarded as radiation detectors is estimated at the level of a few microseconds. The effect of a magnetic field on the single-electron and Andreev conductivity of SINIS structures is studied.**

Keywords: tunnel junctions, superconductor–insulator–normal metal–insulator–superconductor structures, Andreev current, millimeter-wave radiation detectors, electron temperature, electron–phonon interaction, Abrikosov vortex structures

S.A. Lemzyakov [1, a], **M.A. Tarasov** [2, b], **V.S. Edelman** [1, c]
[1] Kapitza Institute for Physical Problems,
Russian Academy of Sciences, ul. Kosygina 2, 119334 Moscow,
Russian Federation
[2] Kotel'nikov Institute of Radio Engineering and Electronics,
Russian Academy of Sciences,
ul. Mokhovaya 11, korp. 7, 125009 Moscow, Russian Federation
E-mail: [a] lemserj@gmail.com, [b] tarasov@hitech.cplire.ru,
[c] vsedelman@yandex.ru

Received 18 December 2024
Uspekhi Fizicheskikh Nauk **195** (7) 759 – 765 (2025)
Translated by S. Alekseev

1. Introduction

Interest in studying superconductor–insulator–normal-metal–insulator–superconductor (SINIS) microstructures is a result of the proposal to use them in radio astronomy as a sensitive element integrated into a planar antenna of a millimeter or submillimeter radiation receiver [1, 2]. The proposal is to connect SINIS electrodes directly to the two halves of the antenna and match the normal strip to the antenna by impedance, so as to have almost all the power of the received radiation absorbed in it, leading to its heating and hence an increase in the tunnel current. To enhance the response to radiation, it is necessary to reduce the volume of normal metal and decrease the temperature T to reduce the heat capacity and weaken the electron–phonon interaction responsible for the outflow of heat from the electron system. However, at the energy of radiation quanta $\hbar\omega \gg kT$, the efficiency of converting the energy received by electrons into current is reduced when the times of electron–electron and electron–phonon interactions become longer than the tunneling time as the temperature decreases [3, 4]. This phenomenon is considered in Section 2.

In Section 3, we describe the results of studying the original metamaterial from a matrix of SINIS-connected elements of semirings with dimensions much smaller than the wavelength. Increasing the total volume of normal SINIS electrodes allowed significantly increasing the efficiency of the photon energy conversion into tunneling current [5]. The response time of such detectors [6] was measured and their noise-equivalent power (NEP) was estimated.

* Joint meeting of the Scientific Session of the Physical Sciences Division of the Russian Academy of Sciences and the Scientific Council of the Kapitza Institute for Physical Problems of the Russian Academy of Sciences, dedicated to the 90th anniversary of the Kapitza Institute for Physical Problems, Russian Academy of Sciences (December 18, 2024) (see *Phys. Usp.* **68** (7) 699 (2025); *Usp. Fiz. Nauk* **195** 747 (2025)).

Section 4 is devoted to the study of the magnetic field effect on the low-temperature SINIS conductivity at low voltages, when the single-electron current and the subgap Andreev current are comparable [7, 8].

2. Nonthermal response to subterahertz radiation

We studied the variation in the SINIS tunnel current under the influence of radiation with an average frequency of 340 GHz, corresponding to the atmospheric transparency window. The radiation receiver is a planar antenna made of two halves connected by a chain of three series-connected SINIS structures, with the superconductivity of the aluminum absorber suppressed by a magnetic Fe impurity. The microwave signal was received through a capacitive coupling between the antenna elements and the SINIS structure. The area of each tunnel junction was 0.25 μm^2, the thickness of the tunnel barrier was 0.01 μm, and the normal-state resistance was $R_n = 3.8$ kΩ. The radiation source was a silicon plate with a deposited nichrome film, whose temperature was varied from ∼ 0.4 K to ∼ 10 K by passing current through the film. The sample was cooled to low temperatures in a dilution cryostat based on a pulse tube [9].

Thermal radiation was incident on the receiver through a diaphragm closed by interference filters with an average frequency of 340 GHz and a width of 45 GHz and 50% transmission at the maximum. When calculating the power incident on the receiver, the effect that interference on the thickness of the silicon plate has on the emitter blackness was taken into account. The characteristics of the filter and emitter were refined in [6] and were taken into account when writing this paper. Figure 1 shows the measurement results at substrate temperatures of 70 and 337 mK and a comparison with the calculation of the single-electron current I_{single} to within 1% at low voltages on the tunnel junction [10],

$$I_{single} = \frac{1}{eR_n}\sqrt{2\pi k T_e \Delta_c}\,\exp\left(\frac{-\Delta_c}{kT_e}\right)\sinh\frac{eV}{kT_e}, \qquad (1)$$

where Δ_c is the energy gap in the superconductor and T_e is the electron temperature in the normal metal.

At $T = 70$ mK, formula (1) provides a good description of the $I(V)$ dependence in the range from 0 to ∼ 0.5 mV at $T_e = 205$ mK. At high voltages, electron cooling manifests itself, leading to a decrease in the current. The higher temperature of the electrons than that of the substrate is caused by their heating by stray radiation penetrating from the room. Such a difference was observed in all the samples of the receiving systems that we studied and was absent in the test structures without antennas placed on the same chips. Under irradiation, the variation in the SINIS current differs sharply from its variation during heating, and the $I(V)$ dependence is not described by formula (1), which is valid for the equilibrium of the electron system. This is direct evidence of a violation of the thermal equilibrium in the electron system.

At $T = 337$ mK, the $I(V)$ dependence is described by formula (1). Thus, as the temperature increases, equilibrium is established in the electron system during irradiation. Knowing T_e, this allows calculating the power absorbed by electrons using the well-known formula for the electron–phonon interaction [11]

$$P_{e\text{–}ph} = \Sigma v\,(T_e^6 - T_{ph}^6), \qquad (2)$$

where Σ is a constant equal to 2.3 nW μm^{-3} K^{-6} and v is the volume of normal metal, equal to ∼ 0.008 μm^3 for three SINIS structures. As a result, at $T_e = 365$ mK, we obtain $P_{e\text{–}ph} \sim 0.015$ pW, which is only ∼ 4% of the power of ∼ 0.4 pW incident on the receiving structure.

The conversion of photon energy into electron energy is a complex multistage process. Photons with a frequency of 340 GHz are absorbed by electrons [12]. In normal metal, electrons with energies in the range of 0–16 K above the Fermi level are then excited, and free states therefore appear with energies in the same range below the Fermi level. Next, energetic quasiparticles generate energetic phonons and electrons, and lower-energy holes are formed. 'Hot' phonons in turn transfer energy to other electrons, and so on. Simultaneously, energy is exchanged in electron–electron interactions. All the described processes are characterized by the times $\tau_{e\text{–}ph}$, $\tau_{p\text{–}h}$, and $\tau_{e\text{–}e}$ of electron–phonon, phonon–electron, and electron–electron interactions. At energy Δ_c for thin aluminum films, $\tau_{e\text{–}ph} = 25$ ns, $\tau_{p\text{–}h} = 37$ ps, and $\tau_{e\text{–}e} = 540$ ns. These times respectively depend on the energy E as E^{-4}, E^{-2}, and $\sim E^{-2}$. They should be compared with the

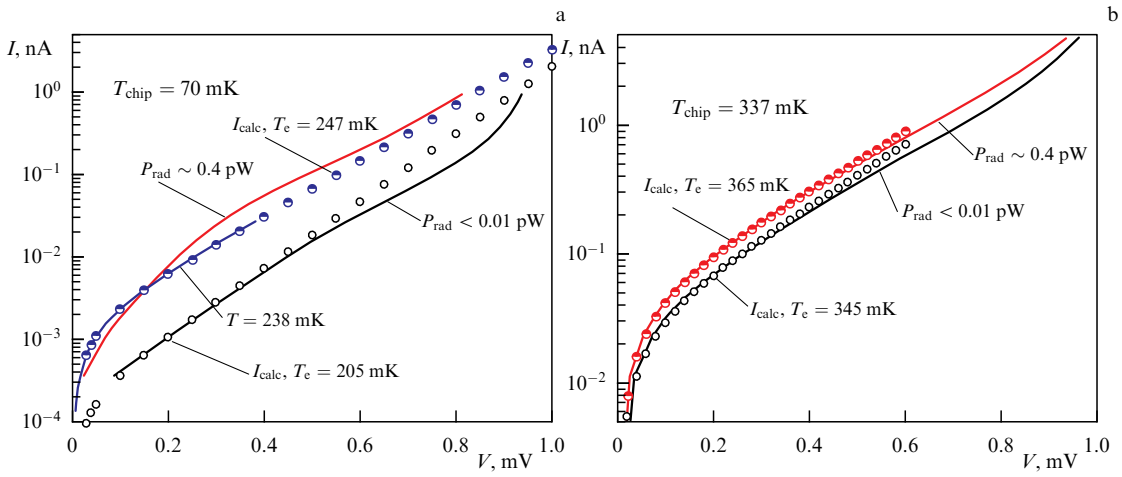

Figure 1. Current-voltage characteristics (I–V) of SINIS structure without irradiation and under irradiation by $P \sim 0.4$ pW with average frequency of 340 GHz at temperature of (a) 70 mK and (b) 337 mK and their comparison with calculated I–V for equilibrium state of electron system and with I–V measured at 0.238 K in the absence of irradiation.

tunneling time of ~ 75 ns during which electrons with energies greater than that of the gap leave the normal metal, and with the travelling time of phonons at junction thickness of the order of a micrometer for ~ 25 ps, some of which are not reflected from the boundary and drop out of the process of equilibrium setting in. Just the escape of phonons can possibly be responsible for the low efficiency of converting the incident power into heating of the electron system. The results in [11] were used in the above calculations.

Qualitative considerations of this sort are clearly not sufficient. For example, already at an electron energy of ~ 2 K, the time $\tau_{e\text{–}e}$ is an order of magnitude longer than all other times. Nevertheless, even at $T_e \sim 0.3$ K, the electron system reaches equilibrium; the problem awaits resolution.

3. Measuring response time of SINIS receivers

According to estimates, the signal rise time when irradiating receivers with SINIS detectors at low temperatures amounts to microseconds. To experimentally determine it, we need a source of a rapidly increasing subterahertz radiation signal and a system for measuring a pulse signal in the microvolt range.

The first measurements are presented in [13]. The measurement scheme is shown in Fig. 2. The emitter is a thin sapphire plate with a deposited nichrome film. When a short current pulse with an amplitude of tens of volts is passed through it, due to its low heat capacity at low temperatures and high thermal conductivity, it heats up in about a microsecond and slowly cools down after the current pulse ends. As a result, a thermal radiation pulse is formed in the shape of a step with a steep front. A bias current of alternately positive and negative polarity, switched between heating pulses, is fed through the receiving SINIS structure. The voltage taken from the SINIS structure is amplified and fed to a digital high-speed oscilloscope, whose output signals are summed by a computer separately for each polarity. To reduce the noise-to-signal ratio at each measurement current, heating pulses are applied many times. Subtracting these accumulated voltages allows suppressing interference from the leading and trailing edges of the electric pulse, which are much higher than the measured signal. Measurements carried out with SINIS structures built into a log-periodic antenna showed that the response rise time for it is 1.8 ± 0.5 μs at $T_e = 0.17$ K.

However, the described technique for generating a radiation pulse has the disadvantage that it requires modeling the variation in the emitter temperature, which cannot be measured directly due to the absence of radiation receivers faster than SINIS structures at low temperatures. It does not allow providing pulses with a fast decay. Therefore, the next step was to use impact ionization avalanche transit-time (IMPATT) diod radiation generators operating at room temperature. They can be gauged using photodiodes, whose signal is amplified by the same amplifier that is used for preliminary amplification of SINIS detector signals. According to measurements in [6], the front of the IMPATT diod radiation pulse has a rise and fall time constant equal to 0.1–0.12 μs. The amplifier contributes another 0.3 μs. There is another component of the delay time, RC, where R is the SINIS resistance and C is the capacitance of the signal transmission line from the cryostat to the room. To reduce this time to fractions of a microsecond, measurements must be carried out at voltages V near Δ_c/e, when the voltage

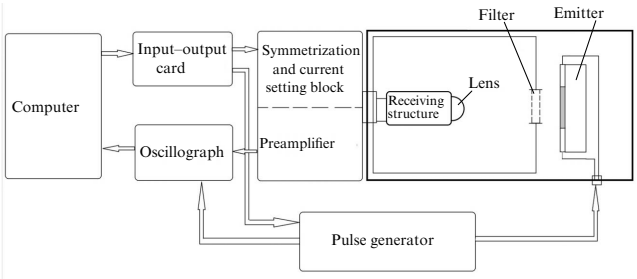

Figure 2. Block diagram of measurement of response to rapidly changing radiation.

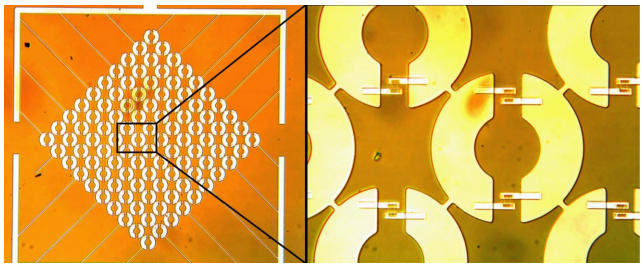

Figure 3. Photograph of parallel metastructure of half-rings connected by pair of SINIS structures.

response δV is small. This requires increasing the probing signal power.

The voltage response $\delta V(P)$ to the IMPATT diod radiation was studied for a metamaterial — a multielement structure of SINIS-connected semirings (Fig. 3). All rings were connected in parallel by direct current. Hereinafter, we call such a structure an MPM (metamaterial parallel matrix). The outer diameter of the rings is 54 μm, much smaller than the wavelength. A square matrix of 100 rings has dimensions of 0.62×0.62 mm^2. The parameters of the superconductor–insulator–normal-metal (NIS) tunnel junctions are as follows: area of 0.4 μm^2, stripes of normal absorber between them of 0.1×1.5 μm^2, and thickness of normal stripes (aluminum with an iron sublayer) of 20 nm. Figure 4 shows the response to the radiation of such a receiver. At a temperature of 0.33 K, the rise time constant is 0.6–0.7 μs, and the fall time is 1.3 μs. At $T \sim 0.1$ K and $T_e \sim 0.2$ K, the MPM's own response time can be estimated by the front at 4 ± 1 μs, and by the fall at 7.5 ± 1 μs. The ratio of times at two temperatures, 0.33 and 0.2 K, is in the range of 4–8.

For a small variation in T_e, the response time determined by the ratio of the heat capacity of the normal metal $C = v\gamma T_e$ (where γ is a material-dependent electron heat capacity constant) to the heat removal due to the electron–phonon interaction (formula (2)) is given by

$$\tau = \frac{\gamma}{6\Sigma T_e^4}, \tag{3}$$

and, at the chosen temperatures, a time ratio of ~ 7 can be expected, which does not contradict the experiment. However, judging by the response amplitude, the condition of small heating of electrons is not satisfied. Apparently, this also determines the difference between the growth and decay times and the time during irradiation of the MPM being the several times longer than the SINIS one with a log-periodic antenna.

Manufacturing the MPM is one of the stages in creating radiation receivers with a large dynamical range. It is ensured

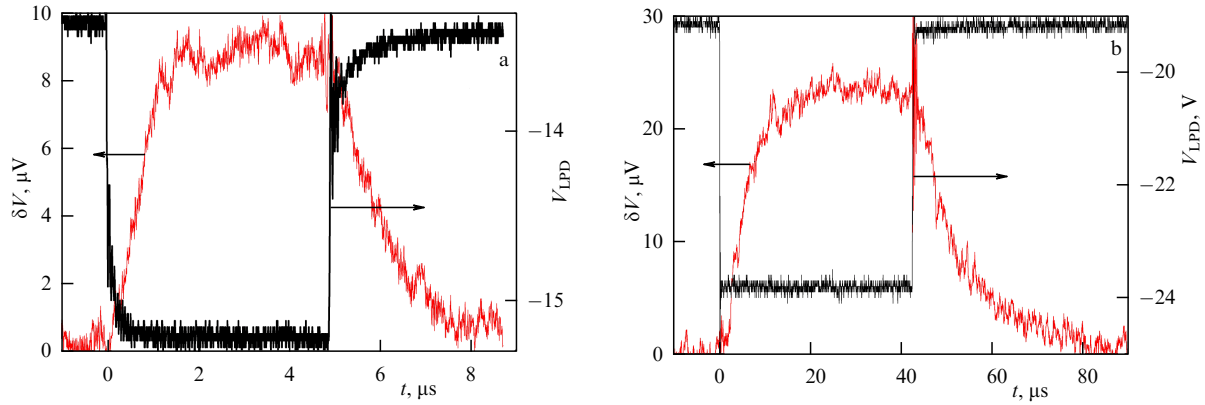

Figure 4. Response of parallel metastructure to pulsed radiation from an IMPATT diod at 350 GHz: (a) $T \approx T_e = 0.33$ K and (b) $T = 0.1$ K, $T_e = 0.2$ K.

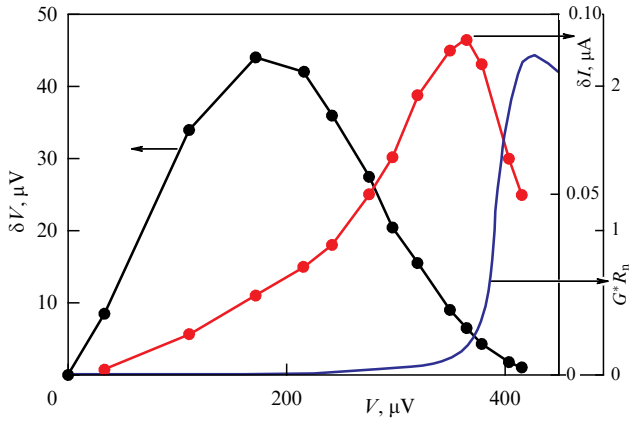

Figure 5. Response of parallel metastructure to radiation with a power of ~ 1 pW and average frequency of 340 GHz.

by the fact that only 1% of the power incident on the receiver arrives at each SINIS structure.

In Figure 5, we show the response δV to thermal radiation with an average frequency of 340 GHz and a power of 1 pW, calculated based on the temperature of the emitter and the geometric parameters of the device. At V near Δ_c/e, when the voltage response is small, the measurements were carried out using the pulse technique described above at several values of the tunnel current in order to increase the signal-to-noise ratio. The heating pulses had a small amplitude and a duration of 0.1 s. This caused no problems in determining the temperature of the emitter and hence the dependence of the radiation power P on time during the current pulse. Control was implemented by ensuring that the dependences $P(t)$ and $\delta V(t)$ normalized to their maximum values coincide. The current response δI was calculated as δVG, where $G = \mathrm{d}I/\mathrm{d}V$ is the SINIS differential conductivity.

It turned out that a large volume of normal metal did not lead to a decrease in sensitivity. Although the lateral dimensions of each NIS junction are only slightly larger than those of the NISs described in the preceding section, and the parameters R_nS determining the tunneling time are almost the same, no obvious signatures of an MSM nonthermal response were observed. Perhaps the differences among the thicknesses of the normal metal films by a factor of two leads to a change in the phonon spectrum: vibrations of the aluminum lattice atoms are coupled to the silicon substrate: the stronger they are, the thinner the metal layer.

The current response turned out to be quite significant. At $P = 1$ pW at the maximum $\delta I = 0.09$ μA, it was $\sim 10\%$ of the total current. The NEP is estimated at $\sim 2 \times 10^{-17}$ W Hz$^{-1/2}$. When measuring currents of the order of a microampere at room temperature, the existing electron components introduce noise an order of magnitude lower. Therefore, MSM receivers are quite acceptable and competitive for ground-based radio astronomy. At the East Asian Observatory (Hawaii), where the astroclimate is good, the atmospheric noise power lies in the range of $(5-10)\times 10^{-17}$ W Hz$^{-1/2}$ in the atmospheric transparency window, with an average frequency of 350 GHz. For the low-temperature transition-edge sensors used in the James Clerk Maxwell Telescope [14] operating there, NEP $\sim 10^{-16}$ W Hz$^{-1/2}$; they have large dimensions of $\sim 1 \times 1$ mm^2 (which is significant for multiplexing when obtaining a multielement image) and a response time of ~ 1 ms, which is two orders of magnitude worse than the MPM one. This time limits the speed of sky scanning.

To conclude this section, we note that MPM structures are resilient: they withstood several thermal cyclings from room to helium temperatures and were preserved under room conditions from 2018 until 2024. The small dimensions of the NIS junctions make them stable even under intense irradiation with bremsstrahlung and gamma-neutron radiation at the Russian Federal Nuclear Center (Sarov) [15].

4. Effect of magnetic field on conductivity of NIS structures

In the first study investigating the effect of a magnetic field on aluminum–aluminum-oxide–aluminum NIS structures with suppressed superconductivity or copper, the deposited aluminum films were found to be type-II superconductors with the upper critical field B_{c2} approximately 3 times greater than the critical field B_c in pure aluminum [16]. In the field normal to the NIS surface with lateral dimensions greater than ~ 1 μm, at $B_{c1} < B_c$, the conductivity increased abruptly by 2–3 orders of magnitude in the field $B_{c2} \approx B_c/2$. As is known, at $B > B_{c2}$, the Abrikosov vortex structure forms in type-II superconductors. The appearance of normal vortex cores leads to a sharp increase in the tunnel current. Based on the values of the critical fields B_{c1} and B_{c2}, we can estimate the correlation length $\xi \approx 115$–150 nm and the magnetic field penetration depth $\lambda \approx 200$–250 nm for the aluminum films of the studied NIS structure.

Research in this field was continued in [7, 17]. In these studies, a test aluminum–aluminum-oxide–copper NIS struc-

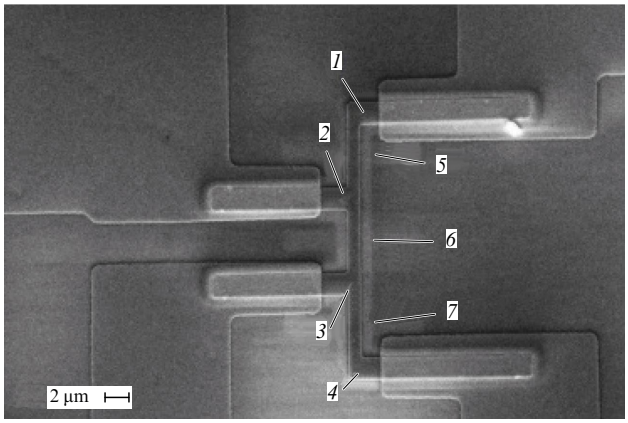

Figure 6. SEM image of SINIS structures on which measurements were carried out. Numbers indicate tunnel junctions *1–4* and suspended bridges made of normal metal *5–7*.

ture was studied (Fig. 6). It contains four copper–aluminum tunnel junctions (*1–4*), connected by a common copper strip deposited on the oxidized surface of aluminum, which is deposited directly on the silicon substrate. In sections *5–7*, the aluminum located under the copper is etched. The film thicknesses are 20 nm (copper) and 80 nm (aluminum), and the respective SIN1 and SIN2 areas are 8 and 10 μm^2. The structure is interesting in that, at a temperature of about 0.1 K at low voltages, when the single-electron current decreases exponentially, the Andreev current appears, which is responsible for the anomalous maximum of conductivity at zero voltage. In [7], as well as in [18], attention was focused on the study of this phenomenon. Later, in [8], a more detailed analysis of the results was carried out, including the influence of the effect of depairing in a magnetic field on the single-electron current (1) and the change in the magnetic field of the two components of the Andreev current. This allowed unambiguously establishing which parameters vary and how they vary under the influence of a magnetic field.

According to the theory in [19], the Andreev current contains two components: I_n, due to the diffusion of a correlated pair in the volume of a normal metal, and I_s, in a superconductor. The obtained expression for the Andreev current $I_{Andreev}$ is

$$I_{Andreev} = I_n + I_s = \frac{\hbar}{e^2 R_n^2 S \nu_n d_n} \tanh \frac{eV}{2kT_e} + \frac{\hbar}{e^2 R_n^2 S \nu_s d_s} \frac{eV/\sqrt{1 - eV/\Delta_c}}{2\pi\Delta_c}, \quad (4)$$

where ν_n and ν_s are the densities of electron states in the normal metal and the superconductor, and d_n and d_s are the layer thicknesses. The measured Andreev current magnitudes are much smaller. The point is that the tunnel barrier is assumed to be homogeneous in theory, but it is not in practice. Therefore, for a two-particle current, the leading contribution is made by those sections of the barrier layer where the probability of tunneling is higher. Based on this, the following formula was used to analyze the experimental results:

$$I_{Andreev} = I_n + I_s = k_n \tanh \frac{eV}{2kT_{eff}} + k_s \frac{eV/\sqrt{1 - eV/\Delta_c}}{\Delta_c}, \quad (5)$$

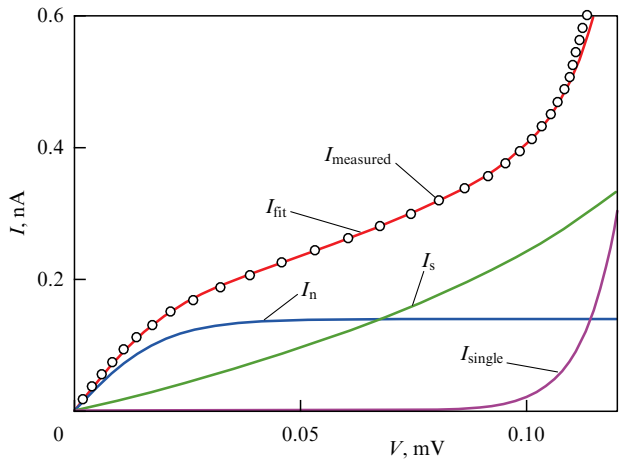

Figure 7. Measured current-voltage characteristic of a SIN structure and its fitting by theoretical models. Fitting uses values $\Delta_c/k = 2.18$ K and $R_n = 29$ Ω, determined from dependence of tunnel current on temperature, and values $k_n = 0.135$ nA, $k_s = 0.32$ nA, $T_{eff} = 0.11$ K, and $T_e = 0.094$ K, at chip temperature $T = 0.09$ K.

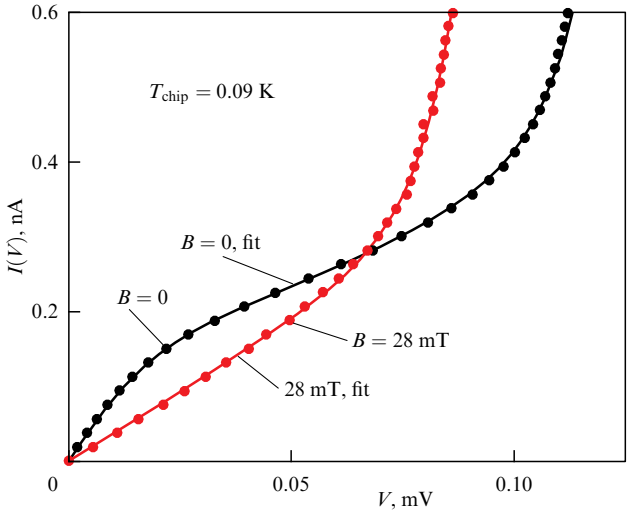

Figure 8. Current-voltage characteristics under the effect of a magnetic field applied in SIN plane.

here, k_n, k_s, and T_{eff} are parameters determined in the course of fitting the experimental results. Figure 7 demonstrates that, at temperature $T \ll T_c$ and voltage on the structure such that the tunnel current is $I \ll V/R_n$ (in practice, this condition is satisfied for $V < \Delta_c/2e$), good agreement with experiment can be achieved.

In a magnetic field, the SINIS conductivity varies similarly to its variation with increasing temperature. The variation is more pronounced in a field directed normal to the SINIS surface than in a field applied in plane. This is because, at lateral sizes of superconducting regions greater than the penetration depth, the distribution is not uniform. Therefore, for the analysis, we used the results obtained with the in-plane field, ensuring that it is uniform in the volume of the superconductor at $d_s < \lambda$. The current-voltage characteristics measured in the presence of a field correspond to formula (5) (Fig. 8). Their variation is similar to the one with increasing temperature, which allows analyzing the effect of the field on the NIS parameters. A constant magnetic field cannot change the temperature. Due to the depairing effect, it leads to a variation in Δ_c (see, e.g., [20]), which affects both

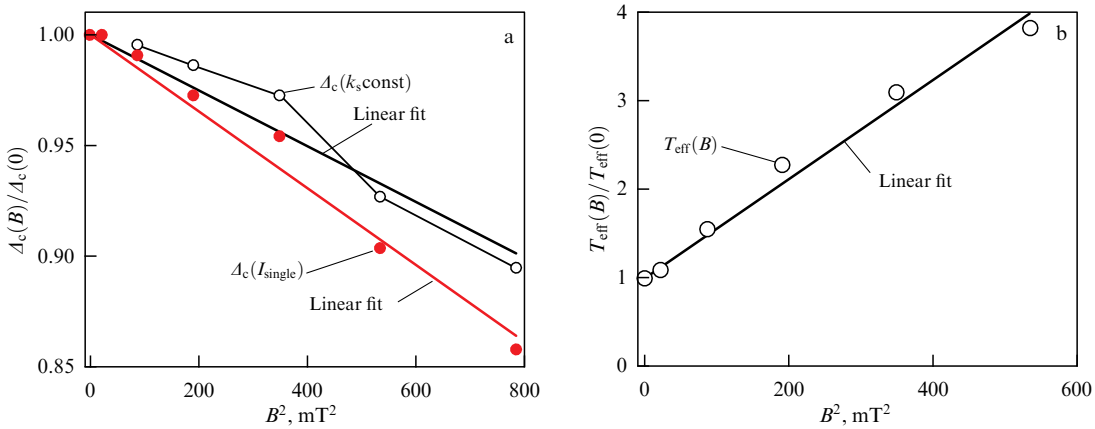

Figure 9. Dependence of (a) Δ_c determined from variation in I_{single} and hence I_s, and (b) change in T_{eff} for I_n, on magnetic field applied in SIN plane.

currents I_{single} and I_s (Fig. 9a). For the I_n current, the field leads to an increase in the effective temperature T_{eff} (Fig. 9b). According to the analysis in [8], the coefficients k_s and k_n do not change, which is natural, because the corresponding expressions in (4) do not contain quantities dependent on the magnetic field.

The dependence of the gap parameter on the field is given by

$$\frac{\Delta_c(B)}{\Delta_c(0)} = 1 - \frac{B^2}{B_0^2}\,. \tag{6}$$

For I_{single}, the characteristic field is $B_0 = 75 \pm 5$ mT, and for I_s, it is 90 ± 8 mT. As shown in [20], where the effect of the field on NIS conductivity made of the same materials with close dimensions was studied, the depairing energy is $\approx \Phi_0/\xi d$, where Φ_0 is the magnetic flux quantum. In our case, the characteristic values of B_0 are close to $\Phi_0/2\xi d_s$.

We note that T_{eff} increases quadratically with the field for $B_0 \approx 13$ mT. If we assume that, by analogy with the effect of the field on the resistance of a normal metal in contact with a superconductor [21], the field is $B_0 = \Phi_0/d_n l_\phi$, where l_ϕ is the length of the drift trajectory with phase loss, we obtain a reasonable value of 8 μm for this parameter in a copper film. The linear size of a normal SINIS film is 12–14 μm.

5. Conclusions

Experiments conducted at the Kapitza Institute for Physical Problems, Russian Academy of Sciences, jointly with the Kotelnikov Institute of Radioengineering and Electronics, Russian Academy of Sciences, showed the promise of planar SINIS detectors for use in ground-based radio astronomy. Fundamental physical properties of SINIS structures at low temperatures were also studied. This paper covers only a small part of the work done. Unfortunately, due to the loss of close contact with theorists who left Russia, we are forced to limit ourselves to qualitative considerations when discussing the results. We hope that this publication will help improve the situation.

Acknowledgments. The authors are grateful to Alexander Fedorovich Andreev for his interest in the work and the useful discussions. We are grateful to the leadership of the Physical Sciences Division of the Russian Academy of Sciences, represented by Academician Secretary V.V. Kveder, for the invitation to present a talk at the scientific session in honor of the 90th anniversary of the Kapitza Institute for Physical Problems, Russian Academy of Sciences. The work was funded within the state assignment of the Kapitza Institute for Physical Problems, Russian Academy of Sciences, and partially by grant 075-15-2024-482 from the Ministry of Science and Higher Education of the Russian Federation.

References

1. Kuzmin L S *Physica B* **284–288** 2129 (2000)
2. Kuzmin L *J. Phys. Conf. Ser.* **97** 012310 (2008)
3. Tarasov M A et al. *J. Exp. Theor. Phys.* **119** 107 (2014); *Zh. Eksp. Teor. Fiz.* **146** 123 (2014)
4. Tarasov M A et al. *IEEE Trans. Terahertz Sci. Technol.* **5** 44 (2015) https://doi.org/10.1109/TTHZ.2014.2379331
5. Tarasov M et al. *J. Appl. Phys.* **125** 174501 (2019)
6. Lemzyakov S A "Vzaimodeistvie SINIS-struktur s submillimetrovym izlucheniem" ("Interaction of superconductor–insulator–normal metal–insulator–superconductor structures with submillimeter radiation"), Thesis of the Candidate of Phys. and Math. Sci. (Moscow: P.L. Kapitza Institute for Physical Problems RAS, 2020)
7. Seliverstov A V, Tarasov M A, Edel'man V S *J. Exp. Theor. Phys.* **124** 643 (2017); *Zh. Eksp. Teor. Fiz.* **151** 752 (2017)
8. Ermakov A B, Tarasov M A, Edel'man V S *Zh. Eksp. Teor. Fiz.* **166** 391 (2024)
9. Edelman V S, Yakopov G V *Instrum. Exp. Tech.* **56** 613 (2013); *Prib. Tekh. Eksp.* (5) 129 (2013)
10. Giaever I, Megerle K *Phys. Rev.* **122** 1101 (1961)
11. O'Neil G C et al. *Phys. Rev. B* **85** 134504 (2012)
12. Devyatov I A, Krutitskii P A, Kupriyanov M Yu *JETP Lett.* **84** 57 (2006); *Pis'ma Zh. Eksp. Teor. Fiz.* **84** 61 (2006)
13. Lemzyakov S A, Tarasov M A, Edelman V S *J. Exp. Theor. Phys.* **126** 825 (2018); *Zh. Eksp. Teor. Fiz.* **153** 992 (2018)
14. Holland W S et al. *Mon. Not. R. Astron. Soc.* **430** 2513 (2013)
15. Atepalikhin A et al., in *IEEE 8th All-Russian Microwave Conf., RMC, Moscow, Russian Federation, 23–25 November 2022* (Piscataway, NJ: IEEE, 2022) p. 23, https://doi.org/10.1109/RMC55984.2022.10079335
16. Tarasov M A, Edel'man V S *JETP Lett.* **101** 740 (2015); *Pis'ma Zh. Eksp. Teor. Fiz.* **101** 740 (2015)
17. Seliverstov A V, Tarasov M A, Edel'man V S *JETP Lett.* **103** 484 (2016); *Pis'ma Zh. Eksp. Teor. Fiz.* **103** 484 (2016)
18. Greibe T et al. *Phys. Rev. Lett.* **106** 097001 (2011)
19. Hekking F W J, Nazarov Yu V *Phys. Rev. B* **49** 6847 (1994)
20. Anthore A, Pothier H, Esteve D *Phys. Rev. Lett.* **90** 127001 (2003)
21. Dikin D A, Black M J, Chandrasekhar V *Phys. Rev. Lett.* **87** 187003 (2001)